JOURNAL OF MATERIALS SCIENCE **34** (1999) 4265–4270

Investigations of the electrical property, diffuse reflectance and ESR spectra of the La-(Fe,Mn)-codoped PTCR $BaTiO_3$ annealed in reducing atmosphere

GANG ER, SHINGO ISHIDA, NOBUYUKI TAKEUCHI
Department of Chemistry and Materials Technology, Kyoto Institute of Technology, Matsugasaki, Sakyoku, Kyoto 606-0962, Japan
E-mail: takeuchi@ipc.kit.ac.jp

Electrical properties of La-(Fe,Mn)-codoped positive temperature coefficient of resistivity (PTCR) $BaTiO_3$ ceramics were studied by combining their diffuse reflectance measurements and electron spin resonance (ESR) spectroscopy. La-(Fe,Mn)-codoped samples showed high durability to reducing atmosphere. It is assumed that Fe and Mn ions segregated in the grain boundary contribute to the density of surface acceptor states, meanwhile localizing electrons in a form of Ti^{3+} and stabilizing the chemisorbed oxygens through La^{3+}-$Mn^{3+,4+}$ or La^{3+}-Fe^{3+} pairs. In addition, ESR signals of Fe^{3+} in annealed samples was intensified above Curie temperature (T_c), indicating that Fe ions still maintained its high valence states (Fe^{3+}) in the grain boundary even after annealing in reducing atmosphere.

1. Introduction

PTCR $BaTiO_3$ ceramics have been widely studied as regards the important roles of minor dopant on their electrical properties, as well as the effect of microstructure and composition of grain-boundary on the PTCR properties during the past decades. Recently, attentions to the degradation of their PTCR properties in reducing atmosphere have been paid [1–3]. The reason for degradation has been attributed to the desorption of chemisorbed oxygen (O^{2-}, O^-), i.e., acceptor states in the grain boundary which formed potential barriers for the occurrence of PTCR property. On the other hand, promotion of PTCR property by doping of minor transition metal ions as acceptors are known, especially Mn, the typical one of which shows the largest improvement of PTCR property [4, 5] and is now being widely used in PTCR thermistors. In addition to the chemisorbed oxygens and barium or titanium vacancies owing to the variation of Ba/Ti ratio and cooling rate [6–8], Mn or the other kinds of transition metal ions acting as acceptor states may also contribute to the potential barrier. We have recently reported that Mn segregation in the grain boundary may enhance the durability to reducing atmosphere, compared to those samples with Mn homogeneously dissolved into the lattice sites [9]. Mn are reported to take high valence states, Mn^{3+} and/or Mn^{4+}, in the grain boundary [4, 10], or form $Mn^{3+,4+}$-donor pairs having high ability of electron trapping [11, 12]. These high valence state Mn ions were reported to change to Mn^{2+} above T_c due to the vanishing of the Jahn-Teller effect as the phase changes from tetragonal to cubic [13], enhancing PTCR properties. Thus it seems important to maintain Mn ion in their high valence states below T_c. Compared to the Mn acceptor, Fe acceptor is also easily segregated in the grain boundary region [14], and its solubility range for semiconductivity is about 0.04 mol %, much lower than $\sim$ 0.1 mol % of Mn [5]. Thus it is expected that Fe-donor pairs may also form at the grain boundary in the case of Fe doping, which will effectively trap electrons and stabilize the chemisorbed oxygen, leading to an enhancement of durability to reducing atmosphere. Moreover, codoping of Mn and Fe acceptors simultaneously will be possible to maintain the PTCR property while improving reducing durability, compared to single doping of each ions. In addition, it will be interesting to study the physical property of multiple-acceptors codoped PTCR $BaTiO_3$ as there have been meager studies about it. This study concerns with preparation and characterization of La-(Mn, Fe)-codoped PTCR $BaTiO_3$ ceramics. Their electrical properties, diffuse reflectance spectra and durability to reducing atmosphere were discussed. The role of Mn, Fe acceptors for PTCR properties and correlation of La with Mn(Fe) were also studied by measuring ESR spectra at various temperatures.

2. Experimental

The process of sample preparation followed the case of Nb(W)-Mn-codoped PTCR $BaTiO_3$ ceramics in our previous publication [9]. High-purity starting materials, $BaTiO_3$ (99.8%, average particle size = 0.6 μm,

Ba/Ti = 0.994, Fuji Titanium Industry Co., LTD., Japan) and 0.4 mol % $La(NO_3)_3$ (water solution) were mixed with 1 mol % of $((C_2H_5O)_4Si)$ by wet-milling for 48 h applying sol-gel coating method [15]. The dopant $La(NO_3)_3$ solution was prepared by dissolving La_2O_3 (99.9%) in 63%HNO_3, then vaporizing the solvent, and once again dissolving in the distilled water. The mixture were dried and calcined at 1050 °C for 2 h in air. 0–0.03 mol % $FeCl_2$ and 0–0.05 mol %$Mn(NO_3)_2$ (water solution) were added to the calcined powder and then ball-milled to get samples with 0.4 mol %La, 0–0.05 mol %Mn and 0–0.03 mol %Fe-codoped-$BaTiO_3$ (hereafter denoted as 0.4La-yMn-zFe, $y = 0 - 0.05$, $z = 0 - 0.03$). After drying, the powder was pressed into disks of diameter 20 × 2 mm. These pellets were finally sintered in air at 1350 °C for 1 h. Samples were then annealed by virtue of an laboratory-available apparatus [16] in flowing ethanol vapor (∼10 kPa) carried by Ar gas at 300 °C for 6–72 h.

Surfaces of samples before and after annealing were carefully polished and applied with In-Ga electrode. The resistivity (R) and relative dielectric constants (ε_r) were measured by the two-probe method using a computer-controlled impedance analyzer (YHP, Model 4192A, Japan). The Cole-Cole plots for the complex impedances measured in the range of 5 Hz to 13 MHz at room temperature (R.T.) were made, and ε_r were calculated at 100 KHz based on the parallel circuit mode. The temperature dependencies of R and ε_r, both of which exhibited abrupt changes around 100 °C, were also examined by slowly heating the samples to about 320 °C in a small electric furnace. The density of surface acceptor states (N_s) was calculated based on Heywang model [17, 18] described as follows:

$$\log R = (e^2 r N_s / 4\varepsilon_0 k \times 10^8) \times (10^8 / 2.303\varepsilon_r T) + \log R_0 \quad (1)$$

$$N_s = 4a\varepsilon_0 k \times 10^8 / r e^2 \quad (2)$$

where r, T, k, e, ε_0 and R_0 represent the average grain size, absolute temperature, Boltzman's constant, electron charge, vacuum permittivity and constant, respectively. Parameter a is a slope of a linear line made up of plotted points for $\log R$ against $10^8/2.303\varepsilon_r T$, which will be shown later in Figs 3 and 4.

Changes in the conduction electron concentration (N_d) with the amount of Fe and Mn were investigated by measuring of diffuse reflectance spectra in the 300–1500 nm wavelength region using Al_2O_3 as a reference. The reflectance spectra were transformed to the absorption spectra using the remission function:

$$f(R_e) = (1 - R_e)^2 / 2R_e \quad (3)$$

where R_e is the reflectance and $f(R_e)$ is proportional to the absorption coefficient (k). It seems worth mentioning that free carriers such as conduction electron shows broad absorption band in the region of visible and infrared region (500−1300 nm), the remission function of which can be expressed as $f(R_e) = A\lambda^n$ ($n = 1.5-3.5$), where λ is the wavelength of absorption light and A is a coefficient proportional to N_d. Thus the relative variation in N_d can qualitatively be followed [9, 16] by detecting the relative change in $f(R_e)$ at certain λ.

ESR spectra were measured on those samples doped with Fe and Mn by X-band ESR spectrometer (JEOL, Model JES-TE 300, Japan) at temperatures ranging from R.T. to 423 K, for the investigation of valence states of Mn and Fe below and above T_c. The central magnetic field was 335 mT, sweep width $\Delta H = 50-250$ mT, and the microwave frequencies were 9.45 GHz for R.T. measurement and 9.21 GHz for temperature dependence measurement, respectively.

3. Results and discussion

3.1. Electrical properties and diffuse reflectance spectra of 0.4La-yMn-zFe-codoped $BaTiO_3$

Samples could be obtained with high relative densities of about 96–97% of their theoretical values. Scanning electron microscope (SEM) showed that average grain size r for 0.4La, 0.4La-0.01Fe, 0.4La-0.03Fe, 0.4La-0.05Mn and 0.4La-0.03Mn-0.02Fe samples were about 4.9, 161.9, 78.0, 47.9 and 58.9 μm, respectively. Doping of Fe or Mn seems to accelerate the grain growth remarkably compared to that of 0.4La sample. This effect is more significant in the case of Fe-doped samples, in which r of 4La-0.01Fe is the largest.

Based on the results of Cole-Cole plots at R.T. for untreated samples and annealed samples, the apparent grain-boundary resistivity (R_{gb}) for as-prepared samples 0.4La, 0.4La-0.01Fe, 0.4La-0.03Fe, 0.4La-0.05Mn and 0.4La-0.03Mn-0.02Fe samples were calculated to be 167.1, 3.19, 164.5, 19.4 Ωcm and about 2×10^7 Ωcm, respectively, while their grain bulk resistivity(R_b) were 22.4, 1.31, 5.26, 9.91 and 5.74 Ωcm respectively. Similarly to the case of 0.4La-0.03Mn-0.02Fe, a complete semi-circular shape of complex impedance was neither obtained in the case of 0.4La-0.05Fe sample, and its R_{gb} and R_b were estimated to be about 8×10^7 and 13 Ωcm, respectively. R_{gb} of both 0.4La-0.03Mn-0.02Fe and 0.4La-0.05Fe samples were about six orders of magnitudes higher compared to that of 0.4La-0.05Mn-sample containing the same total amount (500 ppm) of acceptor, indicating insulation of grain boundary probably attributable to heavy segregation of acceptor Fe in these samples. There were no obvious changes in both R_{gb} and R_b of these samples after annealing at 300 °C for 72 h in ethanol vapor.

The temperature dependences of R were presented in Fig. 1. The PTCR jump, $\log R_{max}/R_{min}$ slightly decreased after annealing in ethanol vapor for 72 h. PTCR jumps in untreated samples were 1.03, 2.44 and 3.05 order of magnitudes, but they changed to 0.95, 2.47, 2.70 orders of magnitudes for 0.4La, 0.4La-0.01Fe and 0.4La-0.03Fe samples, respectively. PTCR jump of 0.4La-0.05Mn sample were 4.03, 3.91 and 3.75 orders of magnitudes after annealing in ethanol vapor for 0, 6, and 72 h, respectively, as shown in Fig. 2. The decreases in the PTCR jump were small in both Fe

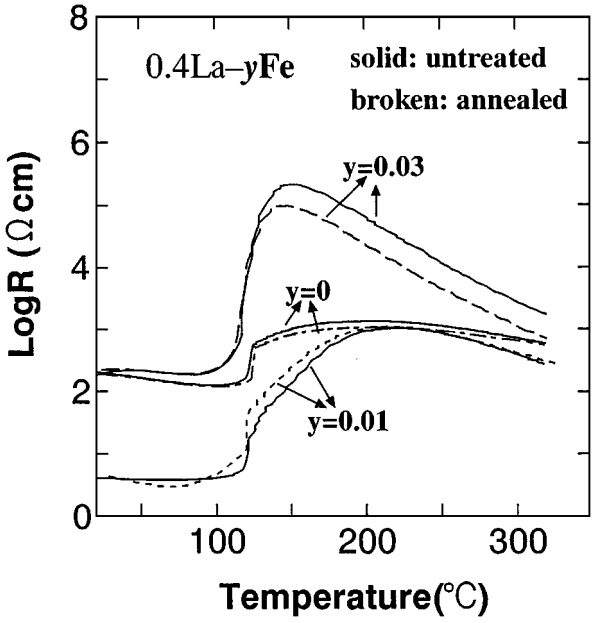

Figure 1 PTCR properties of 0.4La-zFe samples sintered at 1350 °C for 1 h in air (solid line) and annealed at 300 °C for 72 h in ethanol vapor (broken line).

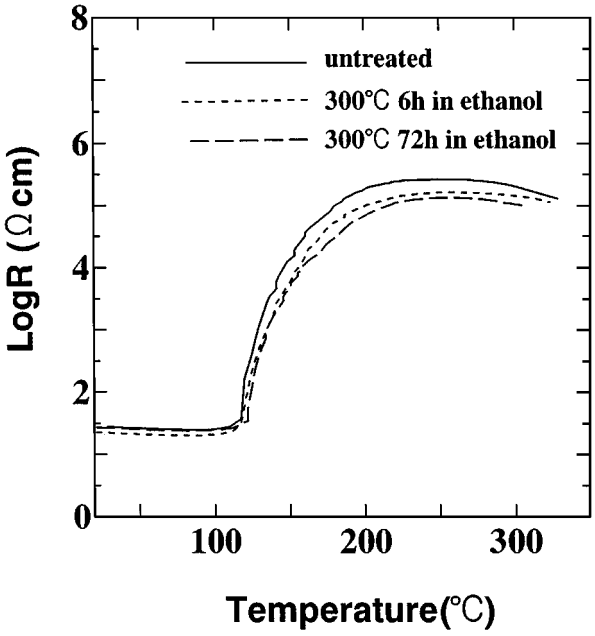

Figure 2 PTCR properties of 0.4La-0.05Mn sample sintered at 1350 °C for 1 h in air (solid line) and annealed at 300 °C for 6–72 h in ethanol vapor (broken line).

and Mn doped samples, indicating that doping of small amount of Fe or Mn in the second step to the calcined powders of La-doped $BaTiO_3$ not only improved the PTCR jump, but also enhanced the durability to the reducing atmosphere.

Changes in $N_s(=1.9048\times10^{12}a/r)$ after annealing were calculated based on the slope a for log R versus $10^8/2.303\varepsilon_r T$ plots [9, 16] (in $T > T_c$ regions), as presented in Figs 3 and 4 for 0.4La-xFe and 0.4La-0.05Mn samples, respectively. Linear relations between log R and $10^8/2.303\varepsilon_r T$ in the $T > T_c$ region were obtained in all samples, indicating the applicability of the Heywang model. Calculated N_s values were listed in Table I. N_s increased with the increasing Fe(Mn) amount, and

TABLE I Variations in $N_s(\times 10^{13}/cm^2)$ of 0.4La-yMn-zFe samples after annealing at 300 °C for 72 h in ethanol vapor

Sample	0.4La	0.4La-0.01Fe	0.4La-0.03Fe	0.4La-0.05Mn
Untreated	0.456	0.832	0.784	1.26
Annealed	0.356	0.760	0.664	0.945

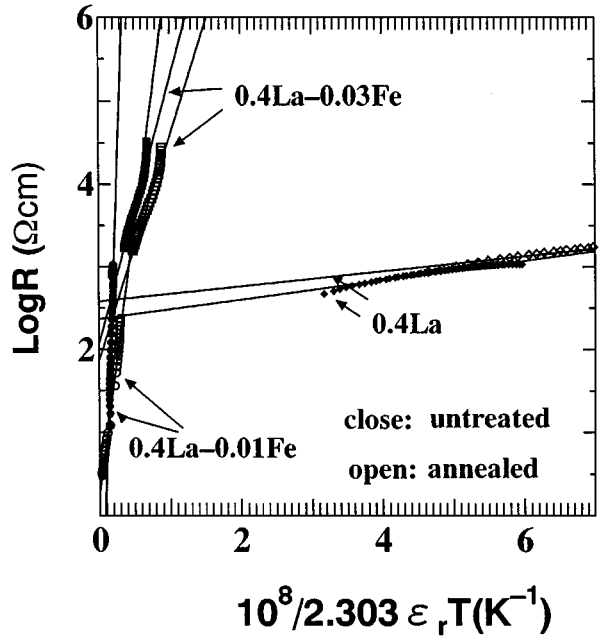

Figure 3 The log R versus $1/\varepsilon_r T$ plots for 0.4La-zFe samples after annealing at 300 °C for 72 h in ethanol vapor (close mark: untreated; open mark: annealed).

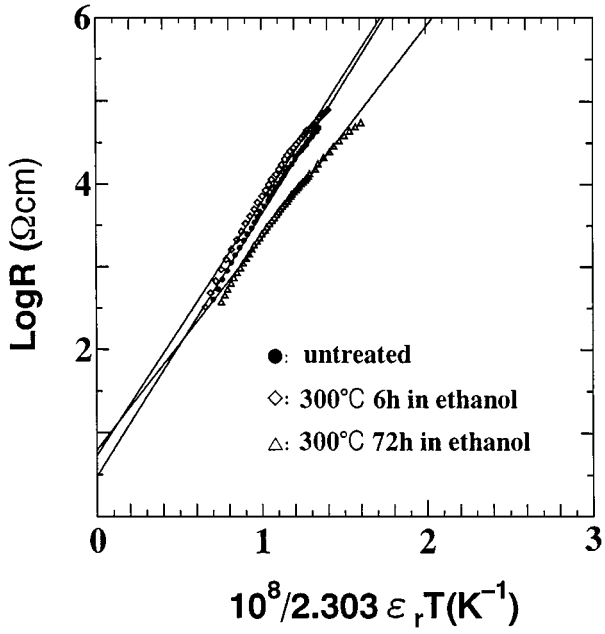

Figure 4 The log R versus $1/\varepsilon_r T$ plots for 0.4La-0.05Mn sample after annealing at 300 °C for 6–72 h in ethanol vapor.

the decrease of N_s after annealing was not obvious in all samples, corresponding to their small degradation in PTCR properties. Fe(Mn) acceptors may exist in the grain boundary, in a form of Fe'_{Ti}-$La^{\bullet}_{Ba}$ or Mn'_{Ti}-$La^{\bullet}_{Ba}$ pairs, which trapped electrons and contribute to the potential barrier in addition to chemisorbed oxygens.

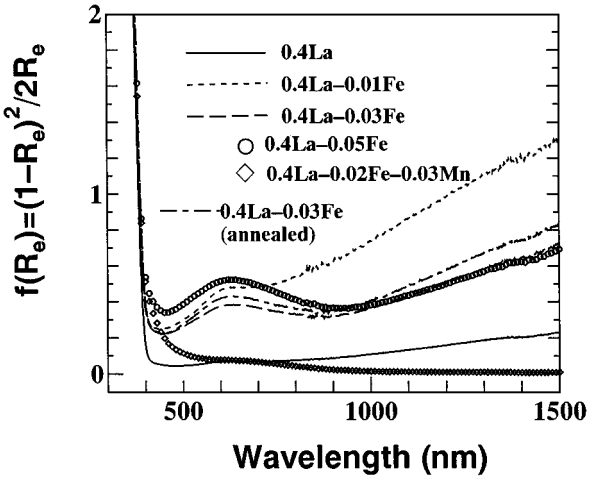

Figure 5 Reflectance spectra of 0.4La-*y*Mn-*z*Fe samples sintered at 1350 °C for 1 h in air and annealed at 300 °C for 72 h in ethanol vapor.

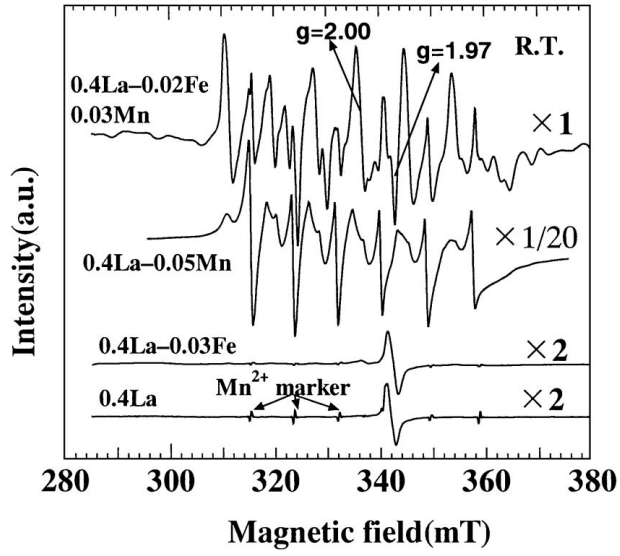

Figure 6 ESR spectra of 0.4La-*y*Mn-*z*Fe samples measured at R.T., frequency ν = 9.45 GHz and sweep width $\Delta H = 50$ mT.

These kinds of acceptors are probably little affected by the reducing agent. This is comparable with acceptors V''_{Ba} or V''''_{Ti} which were produced in quenched $BaTiO_3$ samples after sintering, and a part of PTCR property originated from surface acceptor states V''_{Ba} or V''''_{Ti} did not degrade [8, 19].

In the diffuse reflectance spectra of 0.4La-*y*Mn-*z*Fe samples depicted in Fig. 5, sharp jumps in the ultraviolet region correspond to the absorption edge of the band gap of $BaTiO_3$. A continuous absorption band of conduction carriers in the visible and infrared regions (500–1500 nm) generally decreased in intensity with the increase in acceptors Fe(Mn) amount. The decrease in $f(R_e)$ is consistent with the increase in bulk resistivity, indicating the incorporation of acceptors Fe(Mn) into the lattice, leading to the decrease in N_d. Moreover, $f(R_e)$ showed little change after annealing, corresponding to the unchanged R_b after annealing as mentioned above. This fact indicates that the degradation did not extend to the grain interior under the present annealing condition.

On the other hand, absorption peak around 600 nm which can be ascribed to ${}^2E_{2g} \rightarrow {}^2T_{2g}$ transition of Ti^{3+} with a localized electron [20] appeared in all the samples in addition to the continuous absorption band of the conduction electron. This peak became broader and intensified with increasing acceptor Fe amount, compared to the baseline made up of free carrier absorption. The increase in localized Ti^{3+} amount may be due to Fe'_{Ti}-$La^{\bullet}_{Ba}$ or Mn'_{Ti}-$La^{\bullet}_{Ba}$ pairs enriched in the grain boundary region as mentioned above, which changed the nearby $(Ti^{4+} + e')$-$La^{\bullet}_{Ti}$ to $Ti^{3+} + La^{\bullet}_{Ba}$. In another word, electrons supplied by La donors were localized on Ti sites surrounded by Fe(Mn) acceptors. It is reasonable to consider that, as the segregation of Fe occurred acutely with increasing Fe amount, the broadest peak of Ti^{3+} was observed in 0.4La- 0.05Fe sample. This is consistent with the drastic increase reaching about six orders of magnitudes in its R_{gb}. In the Mn-doped samples, however, localized Ti^{3+} states were much less than that observed in Fe-doped ones, indicating that Mn may dissolve more homogeneously into the $BaTiO_3$ lattice sites than Fe.

3.2. Localized Ti^{3+} states and valence states of Mn(Fe) in 0.4La-*y*Mn-*z*Fe-codoped $BaTiO_3$ detected by ESR spectroscopy

In donor-Mn codoped $BaTiO_3$, Mn dissolved in the interior lattice sites usually forms Mn^{2+} which induce six sharp ESR absorption peaks due to hyperfine splitting of its nuclear spin ($I = 5/2$). However, there may be extra peaks shifted from these normal positions if such Mn^{2+} ions had a distorted coordination [12] or surrounded by higher valence states $Mn^{3+,4+}$, as observed in R.T. ESR spectra of 0.2Nb(0.1W)-0.05Mn codoped samples in our previous results [9].

Fig. 6 shows the R.T. ESR spectra of 0.4La-*y*Mn-*z*Fe samples measured at magnetic field of 335 mT with sweep width of 50 mT. Broad peaks between six sharp peaks were observed in Mn-doped samples, which were assumed to originate from Mn^{2+} ions with distorted La-Mn coordinations or surrounded by high valence states $Mn^{3+,4+}$ as mentioned above. These broad peaks in 0.4La-0.03Mn-0.02Fe sample were relatively more intensive than Mn^{2+} signals in normal positions. The coordination of Mn^{2+} may be more complicated in the grain boundary region, at which La, Mn and Fe ions probably easily segregated together.

A peak at $g = 1.97$ was observed in all the samples except 0.4La-0.05Mn sample, which may be attributed to the localized Ti^{3+} states [21]. The appearance of Ti^{3+} was consistent with the reflectance results stated above. In addition, the peak at $g = 2.00$ may also be assigned to Fe^{3+} absorption, as the wide-scan spectra shown in Fig. 7 supported these assignments. Peaks at $g = 1.62$, 2.00, 2.47, and 5.54 can be attributed to the absorption of Fe^{3+} ions in tetragonal symmetry [22–24], while the sharp peaks at $g = 1.97$ originated from the Ti^{3+} signals. Both the intensities of Fe^{3+} and Ti^{3+} signals increased with increasing Fe amount, corresponding to the increase of Ti^{3+} absorption in diffuse reflectance spectra mentioned above. The same peaks of Fe^{3+} also weakly detected in 0.4La sample, which may be ascribed to the minor Fe impurity (~40 ppm) in the $BaTiO_3$ raw material. Electrons are considered

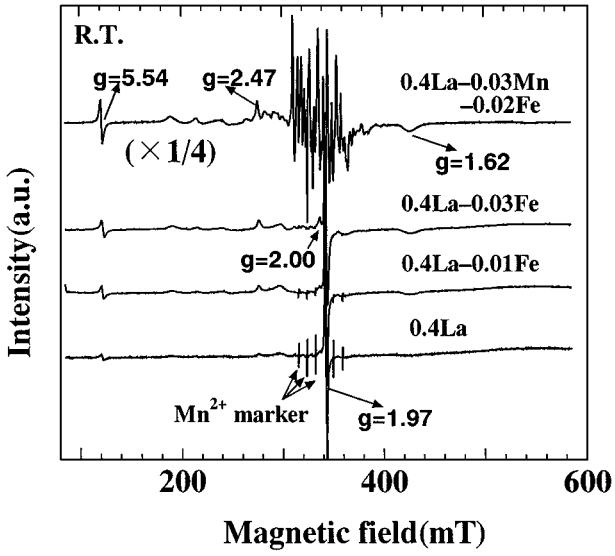

Figure 7 ESR spectra of 0.4La-*y*Mn-*z*Fe samples measured at R.T., frequency ν = 9.45 GHz and sweep width $\Delta H = 250$ mT.

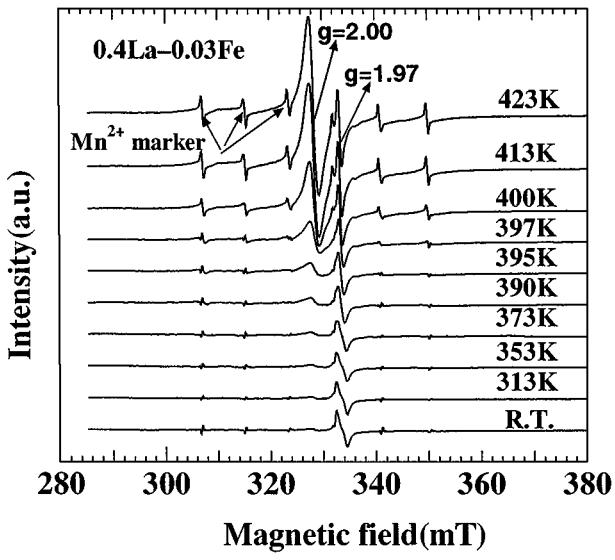

Figure 8 Temperature dependence of ESR spectra of 0.4La-0.03Fe sample measured at frequency $\nu = 9.21$ GHz.

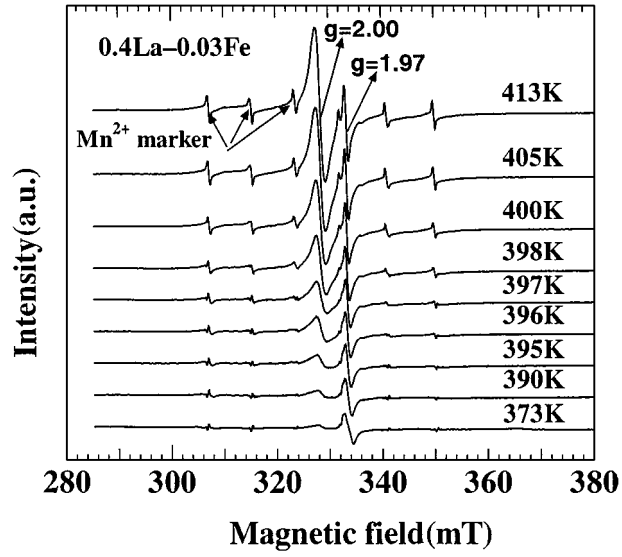

Figure 9 Temperature dependence of ESR spectra of 0.4La-0.03Fe sample measured in the vicinity of T_c at frequency $\nu = 9.21$ GHz.

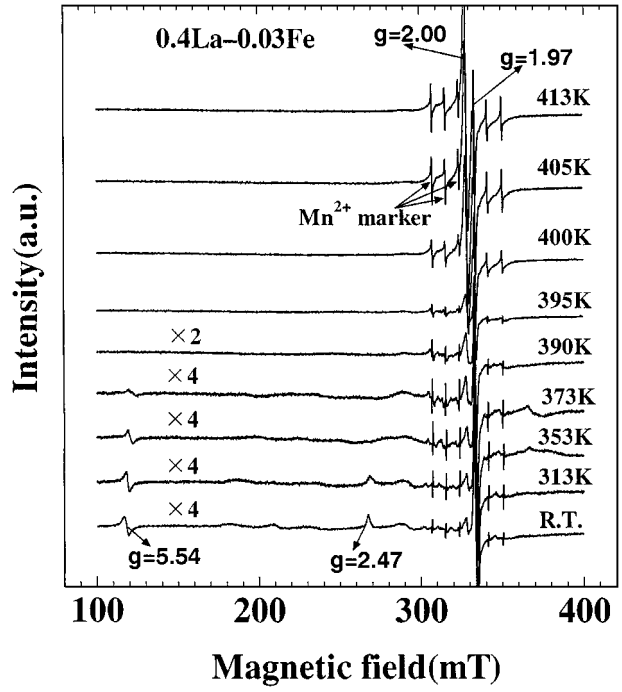

Figure 10 Temperature dependence of ESR spectra of 0.4La-0.03Fe sample measured at frequency $\nu = 9.21$ GHz and sweep width $\Delta H = 250$ mT.

easily to be localized to form Ti^{3+} due to the large segregation of Fe, resulting in a rapid insulation of the grain boundary regions, as observed in the cases of 0.4La-0.03Mn-0.02Fe and 0.4La-0.05Fe samples.

Typical temperature dependence of ESR spectra of annealed 0.4La-0.03Fe sample was shown in Fig. 8. The spectra measured in more detail around T_c were also shown in Fig. 9. Fe^{3+} peak markedly increased in intensity above T_c, and Ti^{3+} peak also gradually increased with temperature. These changes also occurred reversibly, indicating their correlation with the phase transitions from tetragonal to cubic at T_c. Since Fe^{3+} signals were detected at R.T. in all Fe-doped samples, charge valence states of Fe ions may not vary with temperature as proposed in the case of Mn ions. However, the cubic symmetry may favor $3d^5$ electronic structure in high spin states, thus the Jahn-Teller effect in tetragonal phase vanished. As a result, transition probability of $3d^5$ electrons of Fe^{3+} may increase and the absorption peak was intensified. Kutty *et al.* [21, 25] assigned the similar peak($g \approx 2.00$) observed in their La-doped $BaTiO_3$ sample to the V'_{Ba} defect centers, originating from V_{Ba}, which changed to $V'_{Ba} + h^{\cdot}$ above T_c and the PTCR property was enhanced. In the spectra shown in Fig. 10, the other characteristic peaks except $g = 2.00$ of Fe^{3+} which were only detected in tetragonal phase disappeared above T_c, and this phenomenon took place reversibly with the phase transition. Fe^{3+} signals can be detected at the concentration level as low as $10^1 - 10^2$ ppm and the signals increased in intensity with increasing Fe amount in the present samples. Thus, $g = 2.00$ peak detected in their samples is assumed to be attributable to Fe impurities ($\sim 10^1$ ppm) rather than V'_{Ba}. This assumption needs further examinations, but at least the possibility cannot be denied. The Fe^{3+} and

Ti^{3+} peaks were not affected by annealing in the reducing atmosphere, indicating that Fe^{3+} maintained its valence states and Fe'_{Ti}-$La^{\bullet}_{Ba}$ pairs also have high ability of trapping electrons as well as La-Mn pairs.

On the other hand, the increase in both the intensities of Fe^{3+} and Ti^{3+} signals may also be explained by the Ti-O dipole effect. As spontaneous polarization exist in these samples below T_c, Ti-O dipole may absorb a part of microwave energy in a form of heat loss, causing the effective microwave power for ESR absorption to be less than the input power. In fact, Figs 8–10 also indicated that the intensity of Mn^{2+} marker also increased to some extent above T_c as well as Fe^{3+} and Ti^{3+}. Both the dipole effect and the vanishing of Jahn-teller effect contributed to the increase in Fe^{3+} and Ti^{3+} signals, while the latter seems to be more dominant. In a word, the variation in Fe^{3+} intensity is closely related to the phase transition from ferroelectric tetragonal to paraelectric cubic phase above T_c.

These results indicated that acceptors in La-Mn(Fe)-codoped samples maintained their high valence states, i.e., $Mn^{3+,4+}/Fe^{3+}$ and form La-Mn(Fe) pairs in the grain-boundary region. Such types of acceptors were less affected by the reducing agent and possibly stabilized the nearby O^- and O_2^-, thus prohibiting the reaction of O^- and O_2^- with reducing substance which cause degradation of the PTCR property. Therefore, acceptors of Mn(Fe) deliberately enriched in the grain boundary regions as well as donor ions forming donor-acceptor pairs should not only contribute to the improvement in the PTCR jump but also to the durability to the reducing atmosphere.

4. Conclusion

Degradation behaviors of La-(Fe,Mn)-codoped PTCR $BaTiO_3$ ceramics in reducing atmosphere were studied by measuring their electrical properties, their diffuse reflectance spectra, as well as ESR spectra. The following results were obtained:

(1) Doping of Fe and Mn of about 100–500 ppm in the second step to the calcined La-doped $BaTiO_3$ powder is effective not only for improving the PTCR jump but also for enhancing the durability to reducing atmosphere.

(2) Fe and Mn ions segregated to the grain boundary regions in high valence states (Fe^{3+}, $Mn^{3+,4+}$), contributing to the surface acceptor states and inducing stronger attraction with chemisorbed oxygens through La^{3+}-Mn^{3+-4+} or La^{3+}-Fe^{3+} pairs, which can trap electrons and endure the reducing atmosphere. ESR signals of Fe^{3+} were intensified above T_c, which may be correlated with the phase transition from ferroelectric tetragonal to paraelectric cubic phase at T_c.

(3) Localization of electrons in a form of Ti^{3+} was confirmed, especially in Fe-doped samples. These localized Ti^{3+} was intensified with increasing Fe amount and was not affected by the annealing, which is probably related to the high segregation of Fe ion in the grain boundary.

References

1. H. IGARASHI, S. HAYAKAWA and K. OKAZAKI, *Jpn. J. Appl. Phys.* **20**(20-4) (1981) 135.
2. H. ALLAK, G. RUSSELL and J. WOODS, *J. Phys., D: Appl. Phys.* **20** (1987) 1645.
3. A. HASEGAWA, S. FUJITSU and H. YANAGIDA, *Seramikkusu Ronbunshi* **97** (1989) 549.
4. H. UEOKA, *Ferroelectrics* **7** (1974) 351.
5. H. IHRIG, *J. Amer. Ceram. Soc.* **64** (1981) 617.
6. J. DANIELS and R. WERNICKE, *Philips Res. Rep.* **31** (1976) 544.
7. Y. M. CHIANG and T. TAKAGI, *J. Amer. Ceram. Soc.* **73** (1990) 3286.
8. D. C. SINCLAIR and A. R. WEST, *J. Mater. Sci.* **29** (1994) 6061.
9. G. ER, S. ISHIDA, K. YAMAZAKI and N. TAKEUCHI, *Seramikkusu Ronbunshi* **105** (1997) 675.
10. Y. M. CHIANG and T. TAKAGI, *J. Amer. Ceram. Soc.* **73** (1990) 3278.
11. D. Y. WANG and K. UMEYA, *ibid.* **74** (1991) 280.
12. F. REN and S. ISHIDA, *J. Ceram. Soc. Japan* **103** (1995) 759.
13. J. H. LEE, S. H. KIM and S. H. CHO, *J. Amer. Ceram. Soc.* **78** (1995) 2845.
14. S. B. DESU and D. A. PAYNE, *ibid.* **73** (1990) 3391.
15. F. A. SELML and V. R. W. AMARAKOO, *ibid.* **71** (1988) 934.
16. G. ER, N. TAKEUCHI, S. ISHIDA, K. HOSOKAWA, K. YAMAZAKI, N. KITOH, Y. NABIKA and H. NIIMI, *J. Ceram. Soc. Japan* **104** (1996) 1091.
17. W. HEYWANG, *Solid-State Elec.* **3** (1961) 51.
18. M. KUWABARA, *ibid.* **27** (1984) 929.
19. D. C. SINCLAIR and A. R. WEST, *J. Amer. Ceram. Soc.* **78** (1995) 241.
20. M. NAKAHARA and T. MURAKAMI, *J. Appl. Phys.* **45** (1974) 3795.
21. T. R. N. KUTTY, P. MURUGARAJ and N. S. GAJBHIYE, *Mater. Lett.* **2** (1984) 396.
22. K. A. MULLER and R. S. RUBINS, *Phys. Rev.* **135** (1964) A86.
23. A. W. HORNIG, R. C. REMPEL and H. E. WEAVER, *J. Chem. Phys. Solids* **10** (1959) 1.
24. D. J. A. GAINON, *Phys. Rev.* **134** (1964) A1300.
25. N. S. HARI, P. PADMINI and T. R. N. KUTTY, *J. Mater. Sci. Mater. Elec.* **8** (1997)15.

Received 16 March 1998
and accepted 3 March 1999